Research Square

Preprints are preliminary reports that have not undergone peer review.
They should not be considered conclusive, used to inform clinical practice,
or referenced by the media as validated information.

# Cross-scale evolution law and damage mechanism of voids in longwall goaf

**Liang LI**

2024919@imust.edu.cn

Inner Mongolia University of Science and Technology, Inner Mongolia

**Jianwei LI**

Inner Mongolia University of Science and Technology, Inner Mongolia

**Jian CAO**

Inner Mongolia University of Science and Technology, Inner Mongolia

**Xuwei MAO**

Inner Mongolia University of Science and Technology, Inner Mongolia

**Xisheng WANG**

Inner Mongolia University of Science and Technology, Inner Mongolia

**Xiaoshen XIE**

Inner Mongolia University of Science and Technology, Inner Mongolia

**Xinyuan TIAN**

Inner Mongolia University of Science and Technology, Inner Mongolia

**Article**

**Keywords:** longwall goaf, voids, spatiotemporal distribution characteristics, evolution law, damage mechanism

**Posted Date:** November 4th, 2026

**DOI:** https://doi.org/10.21203/rs.3.rs-11317657/v1

**License:** This work is licensed under a Creative Commons Attribution 4.0 International License.
Read Full License

**Additional Declarations:** Competing interest reported. The authors declare no conflict of interest.

# Cross-scale evolution law and damage mechanism of voids in longwall goaf

**LI Liang[1,2,3,4*], LI Jianwei[1,2,3,4], CAO Jian[1,2,3,4], MAO Xuwei[1,2,3,4], WANG Xisheng[1,2,3,4], XIE Xiaoshen[1,2,3,4], TIAN Xinyuan[1,2,3,4]**

**[*]Corresponding author: Li Liang. Email: 2024919@imust.edu.cn**

1. School of Mining and Coal, Inner Mongolia University of Science and Technology, Inner Mongolia, Baotou 014010, China;
2. Inner Mongolia Key Laboratory of Mining Engineering, Baotou 014010, Inner Mongolia, China;
3. Inner Mongolia Research Center for Coal Safety Mining and Utilization Engineering and Technology, Baotou 014010, Inner Mongolia, China;
4. Inner Mongolia Cooperative Innovation Center for Coal Green Mining and Green Utilization, Baotou 014010, Inner Mongolia, China

**Abstract:** Under the background of the "dual carbon" strategy, the resource-oriented and high-value utilization of coal-based solid wastes has become the core direction of green transformation in the coal industry. As the key spatial carrier for the in-situ disposal of underground solid wastes, the resource potential of large goaf areas urgently needs to be systematically exploited. Accurately grasping the evolution law and damage mechanism of voids in goaf is a key breakthrough for resolving the coordinated development dilemma of "safe and efficient production—in-situ solid waste disposal—ecological environment protection" in coal mining. Therefore, this paper combines transient electromagnetic (TEM) detection with physical model tests to systematically investigate the spatiotemporal distribution characteristics, cross-scale evolution law and damage mechanism of voids in longwall goaf. The results show that: The void development degree in longwall goaf decreases with the increase in vertical distance from the coal seam following a polynomial function. Controlled by the deformation of the mining-induced lower key stratum, the caved rock mass in goaf undergoes a dynamic evolution process of "caving bulking—deformation contraction—full compaction", and the spatiotemporal evolution of voids in the caved zone is highly coupled with the fracture movement of the lower key stratum and the stress distribution of the floor, exhibiting an obvious three-stage variation characteristic. The void development in the caved zone is characterized by significant zonal differentiation, prominent boundary effects and remarkable control by overburden movement, among which roof structure movement and stress transfer are the direct inducements driving the dynamic variation of voids in the caved zone. Furthermore, it is revealed that the voids in goaf serve as the deformation space for the continuous instability of the overburden and ground surface. The damage effects are mainly manifested in two aspects: inducing continuous large deformation of the lower key stratum structure and generating residual subsidence damage, and the occurrence mechanisms of the two types of damage are clarified. The research results can provide theoretical support and reference for the efficient utilization of goaf space resources in longwall mining and the prevention and control of mining-induced damage.

**Keywords:** longwall goaf; voids; spatiotemporal distribution characteristics; evolution law; damage mechanism.

## 1. Introduction

China is the world's largest coal-producing and coal-consuming country. In 2025, the national coal output reached 4.66 billion tons, accounting for 51.5% of the global total output and 56% of the global energy consumption, and coal remains the largest source of the current energy supply [1]. In the underground mining mines, which account for 95% of the coal mines nationwide, longwall mining with the fully caving method is commonly used to manage the goaf roof. After longwall caving mining, the void system formed by the mutual stacking of broken rock masses in the goaf evolves continuously and dynamically, and is characterized by strong concealment, significant spatial distribution heterogeneity and poor structural stability, which in turn brings about a series of

engineering and environmental problems, such as the formation of large goaf areas, massive surface stacking of coal gangue and ecological environment damage. The voids in goaf serve not only as a natural waste-storage carrier but also as the deformation space for the continuous damage of the overburden structure. Their spatiotemporal evolution directly restricts the accurate evaluation of the storage capacity of in-situ gangue storage in goaf, the long-term stability of backfilling structures and the effectiveness of mining-induced damage prevention and control, and has become one of the key scientific issues restricting the popularization and application of green mining technologies. Guided by the "dual carbon" strategy, the resource-oriented and high-value utilization of coal-based solid wastes has become the core development direction of the green and low-carbon transformation of the coal industry. As the core spatial carrier for the source disposal of underground solid wastes, the resource utilization potential of large goaf areas urgently needs to be systematically exploited and released. Therefore, systematically revealing the spatiotemporal evolution law and damage mechanism of voids in goaf is an important breakthrough for resolving the coordinated development dilemma of "safe and efficient mining—source disposal of solid wastes—ecological environment protection", and is of important theoretical and engineering significance for promoting the resource-based utilization of goaf space and the prevention and control of mining-induced damage [2,3].

Academician Qian Minggao pointed out in the scientific connotation of green mining that "green mining should transform the study of the influence of rock mass movement on mine pressure at the working face into the study of the influence of post-mining rock mass movement on the voids formed in the rock mass and their seepage law for gas and liquid, as well as the feasibility of re-forming rock mass structures to protect the ground surface" [4] Research on the void evolution of longwall goaf involves multiple green mining issues, such as backfilling for subsidence reduction, simultaneous extraction of coal and gas, and water-preserved coal mining, and has yielded abundant achievements both at home and abroad. In terms of the failure movement and fracture development of mining-induced rock mass, the general understanding of "three horizontal zones and three vertical zones" has been established. Regarding the spatial development morphology of mining-induced fractures, the code for coal mining under buildings, water bodies and railways (the "three-under" regulation) specifies that the water-conducting fracture zone exhibits a "saddle shape"; Yuan et al.[5] and Li et al. [6] put forward multiple spatial morphologies describing mining-induced fracture evolution, such as the “ring-shaped fracture body” and the “elliptic paraboloid zone”. Xu, J. L. [4,7] established a correlation model between key stratum deformation and goaf morphology based on field measurement analysis. Wang, B. F. [8] quantitatively analyzed the zoning characteristics of mining-induced fractures in the overburden of shallow composite goaf using fractal geometry theory, and provided the fractal dimensions of the fracture network in each fracture zone as well as corresponding zonal treatment schemes. Li, H. Y. [9] quantitatively described the spatiotemporal evolution law of goaf fractures using similar simulation tests and analytical theory, concluding that the medium- and high-angle transition zone is the main region for implementing gas drainage engineering. Zhang, H. Z. [10], based on the analysis of in-situ rock mass measurement data from the former Soviet Union, obtained the variation law of cavities and voids in goaf, holding that cavities and voids mainly appear within a range of 0.4 times the mining depth above the roof in the vertical direction, and that their quantity follows a logarithmic or linear distribution with the mining-thickness ratio and the distance from the working face boundary in the horizontal direction. Hu, S. Y. [11] revealed based on the discrete element method that both voids within caved rock mass and

voids in force chains show bimodal distribution characteristics. It is concluded that with increasing compression, the void ratio of caved rock mass decreases linearly due to force-chain breakage, reorganization and rock-block sliding. Zhang, C. [12] and Hu, S. Y. [13] investigated the evolution of fracture aperture and permeability during goaf compaction, as well as the stress, void ratio and crushing ratio of broken rock mass, by discrete element numerical simulations and laboratory tests. Wolf, K. H. [14] and Miao, X. X. [15] obtained the distribution law of porosity and permeability during gangue compaction in goaf based on field observations and simulation results.In terms of void damage research, Deng, K. Z. [16] concluded that residual subsidence of old goaf is mainly induced by voids in mining-induced fractured rock mass, and proposed a calculation method for the residual subsidence coefficient. Feng, G. R. [17] analyzed the damage influence range of roof strata in longwall goaf using a simplified plane mechanical model, and derived analytical expressions for the heights of the broken caving zone and damage disturbance zone. Li, Q. S. [18] established a damage dissipation model relating the damage coefficients of different subzones in the overburden "three zones" to mining space through field measurements and simulations, and stated that source-based damage reduction at the mining end is a fundamental and effective control measure. Qu, Q. D. [19] proposed the void-volume conservation theory for surface subsidence control in backfill mining and derived the calculation formula of the surface subsidence basin. Guo, W. B. [20] adopted the fractal method to construct a void ratio analysis model for mining-affected zones, and put forward a multi-segment treatment scheme for goaf and corresponding engineering disposal methods for each segment. Yang, K. [21] revealed the "three-stage and three-space" dynamic evolution law of overburden in thick coal seam mining via similar simulation tests. Considering the good matching between the disposal demand of coal-based solid waste and the key spaces formed by overburden movement during coal extraction, a multi-layer collaborative grouting and backfilling system of "lower supporting—middle consolidating—upper controlling" was constructed. Chen, S. J. [22], Guo, G. L. et al. [23] carried out goaf grouting reinforcement under different engineering backgrounds and objectives, and achieved certain subsidence reduction effects. Their outcomes provide reliable theories and methods for investigating void evolution laws and damage mechanisms of old goaf under diverse engineering geological conditions.

The above studies have analyzed the void evolution in goaf and the damage mechanism of the overburden and ground surface from multiple perspectives, promoting the development of mining damage control theory and technology. In early subsidence-area land development and treatment projects, the backfilling properties of coal-based solid waste materials have also been applied; however, most of these are passive post-mining treatment methods for surface protection and subsidence-area development and utilization. Owing to the complex and diverse mining geological conditions and mining methods, the limitation of test conditions, and the complexity of the goaf formation process in longwall mining, the research system on the void evolution law and damage mechanism of goaf is still immature, which restricts the development and application of relevant technologies. Therefore, this paper combines transient electromagnetic (TEM) detection with physical model tests to analyze the spatial distribution characteristics, cross-scale evolution law and damage mechanism of voids in longwall goaf. The research results enrich the green mining technology system and contribute to resolving the tripartite coordination problem of the efficient utilization of goaf space resources, source-based large-scale disposal of coal-based solid wastes and mining damage control, which is of important theoretical and practical significance for the green,

low-carbon and circular development of the coal industry.

# 1 Engineering geological conditions

A certain coal mine mines the No.3 coal seam as its main seam, with an average thickness of 6.0 m. The seam is simple in structure and belongs to a stable thick coal seam, with a hardness coefficient of 0.3–0.5. The main coal-bearing strata in the minefield are the Upper Carboniferous Taiyuan Formation and the Lower Permian Shanxi Formation. The test working face is located in a broad and gentle syncline, with a formation dip angle of 3°–9° (average about 6°), generally higher in the west and lower in the east; influenced by the syncline structure, both ends of the working face are slightly higher while the middle is slightly lower. The floor elevation of the coal seam is +218–244 m, the corresponding surface elevation is +546.0–+616 m, and the cover thickness is 302–398 m. The stratigraphic column of the roof and floor strata is shown in Figure 1. The surface is a mountainous and hilly landform with seasonal gullies. The test working face is 165 m wide and 870 m long, located in the No.3 mining district in the north-central part of the minefield. Coal pillars of 50 m are reserved between the east and west boundaries and the development roadways, a 10 m coal pillar is reserved between the southern intake airway and the adjacent working face, and the north side adjoins the reserved subsequent working face. The working face adopts the retreating fully mechanized top-coal caving mining method, and the fully caving method is used to manage the roof.

| Lithology | Column | Thickness /m | Elevation /m | Key stratum /m |
|---|---|---|---|---|
| medium sandstone | | 17.2-20 | 347.1 | Key stratum |
| sandy mudstone | | 42.9-47.3 | 302 | |
| siltstone | | 5.6-6.0 | 296.2 | |
| medium sandstone | | 2.1-2.8 | 293.75 | |
| No.1Upper coal seam | | 0.3-0.4 | 293.4 | |
| sandy mudstone | | 9.6-10.2 | 283.5 | |
| siltstone | | 2.1-2.8 | 281.05 | |
| sandy mudstone | | 2.9-3.5 | 277.85 | |
| No.1 coal seam | | 0.4-0.5 | 277.4 | |
| sandy mudstone | | 3.1-4.0 | 273.85 | |
| fine sandstone | | 2.6-3.2 | 270.95 | |
| No.2 coal seam | | 0.5-0.6 | 270.4 | |
| sandy mudstone | | 2.8-3.5 | 267.25 | Lower subkey stratum |
| siltstone | | 2.0-2.6 | 264.95 | |
| fine sandstone | | 4.0-5.5 | 260.2 | |
| medium sandstone | | 4.2-4.7 | 255.75 | |
| silty mudstone | | 4.0-4.6 | 251.45 | |
| mudstone | | 1.3-1.6 | 250 | |
| No.3 coal seam | | 5.2-6.6 | 244.1 | |
| fine-grained sandstone | | 1.2-1.5 | 242.75 | |

Figure 1 Stratigraphic column of the roof and floor strata at the test working face

# 2 Detection of void distribution law in goaf

## 2.1 Detection principle and scheme

(1) Detection principle Considering the surface geophysical prospecting environment of the test working face, the transient electromagnetic method (TEM) was selected to detect the void distribution law in goaf. The transient electromagnetic method is an electromagnetic-induction-based detection method. Its principle is based on Faraday's law of electromagnetic induction: an ungrounded loop or electrode is used to transmit a pulsed primary electromagnetic field to the detection target, and then a coil or grounded electrode is used to observe the spatial and temporal distribution of the secondary electromagnetic field generated by the underground eddy currents induced by the pulsed electromagnetic field, so as to solve the relevant geological problems. As a time-domain electromagnetic method, the transient electromagnetic method has been widely applied to the detection of goaf, karst and water-richness of aquifers.

(2) Detection scheme A total of 21 main survey lines for ground transient electromagnetic detection were designed within the range of the working face, and 23 auxiliary survey lines were arranged near the main survey lines, giving a total of 44 TEM survey lines and 1806 TEM physical measuring points, with a total detection area of 40484.4 m², as shown in Figure 2. The FCTEM100-1 high-resolution transient electromagnetic system was adopted, which consists of a TEM main console, a towed transmitting–receiving coil, and data processing and imaging software.

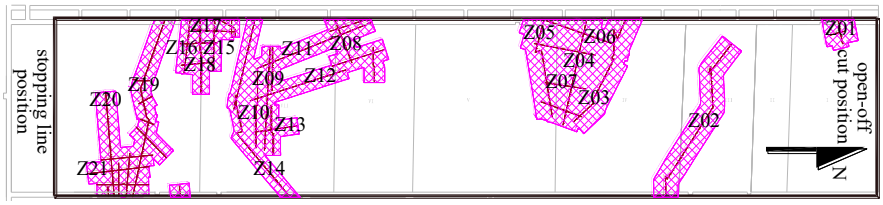



Figure 2 Layout of survey lines and total detection range of the test working face

The raw data signals collected in the field were preprocessed by means of extreme value elimination, wavelet denoising, smoothing filtering, data fitting and windowing sampling, so as to realize signal screening and elimination and noise suppression. Then, the electrical property distribution characteristics of each stratum were obtained through inversion, and the apparent resistivity profile results and the apparent resistivity slice results at different depths were plotted. Combined with the verification results of the high-density resistivity method in this area, the apparent resistivity parameters of different strata/geological bodies within the range of the working face were determined, as shown in Table 1.

Table 1 Apparent resistivity parameters of different strata/geological bodies

| Stratum | Lithology | Apparent resistivity $\rho_s$/Ω·m |
|---|---|---|
| Quaternary overburden | Loess, silty clay, gravelly silty clay, etc. | 80～180 |
| Bedrock layer | Sandy mudstone, limestone, etc. | 50～80 |
| Coal seam | Coal | 80～160 |
| Void anomaly zone | Void anomaly zone (low resistivity, water-bearing) | 20～50 |
| | Void anomaly zone (high resistivity, water-free) | 80～150 |

## 2.2 Void distribution law in goaf

(1) Analysis of electrical property characteristics of strata in goaf

Based on the known geological data of the working face, such as boreholes and hydrology, the special morphology and spatial position relationship of the anomaly zones, the electrical property characteristics of the strata and the resistivity variation law of the surrounding strata, combined with whether the anomaly zones present typical morphological features such as banded, massive or discontinuous shapes, the apparent resistivity slices and geological interpretation map of the test working face at the elevation of 250 m were obtained, as shown in Figure 3. By successively obtaining the slice data at different elevations, the void distribution law in the goaf of the test working face can be comprehensively inferred.

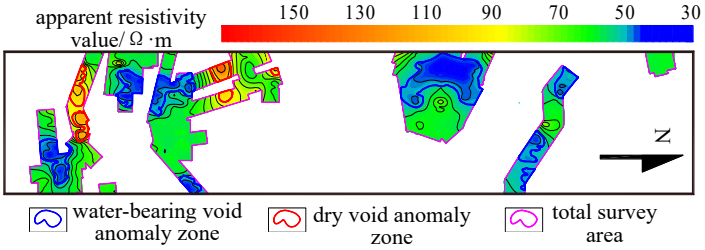



Figure 3 Apparent resistivity slices and geological interpretation at the elevation of 250 m

(2) Void distribution law in goaf

According to the apparent resistivity section results of each TEM survey line, the apparent resistivity values at the elevations of 250, 255, 260, 265, 270, 275 and 280 m were extracted respectively. Taking the cross-sectional area of each anomaly zone as the characteristic value of void development in goaf, the cross-sectional areas of the anomaly zones at each elevation were statistically analyzed, and their variation curves along the vertical direction were plotted, as shown in Figure 4. Through data fitting, the void distribution law in longwall goaf was obtained, i.e., the void development degree in goaf decreases in a polynomial function manner with the increase in the vertical distance from the coal seam.

$$S_c = 0.43z_c^3 - 18.02z_c^2 - 176.68z_c + 10778.63 \quad (1)$$

where $S_c$ is the area of the detected void anomaly zone, in m²; and $z_c$ is the vertical distance from the coal seam, in m.

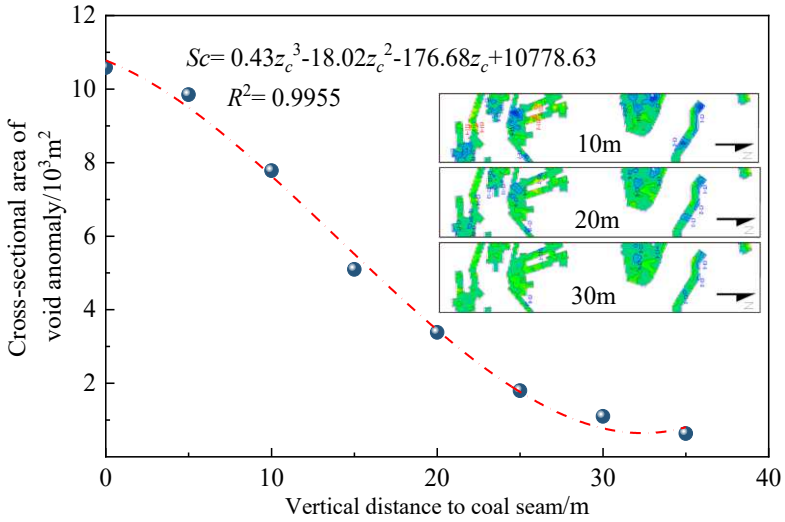



Figure 4 Vertical variation curve of the void development degree in the goaf

# 3 Cross-scale evolution law of voids in goaf

## 3.1 Test scheme

Taking the test working face as the engineering background and based on the similarity theory, the geometric similarity ratio was determined as 1/100. A plane stress model with dimensions of 300 cm × 20 cm × 150 cm (length × width × height) was built using materials with mechanical properties similar to those of the prototype, combined with image binarization processing, measurement and statistical techniques, to quantitatively analyze the whole process of overburden deformation, fracture, movement and the formation and evolution of voids in the caved zone during the advancing process of the working face. To reduce the boundary effect, boundary coal pillars of 30 m were reserved at both ends of the model, and the mining was carried out cyclically from left to right according to the time similarity ratio. During mining, stress monitoring points were continuously arranged on the floor along the advancing direction, and displacement observation lines were arranged at a position 22 m above the roof of the model coal seam, with a measuring point spacing of 20 m. A DH3816N static resistance strain gauge was used to record the floor load variation and roof displacement variation of the working face, as shown in Figure 5.

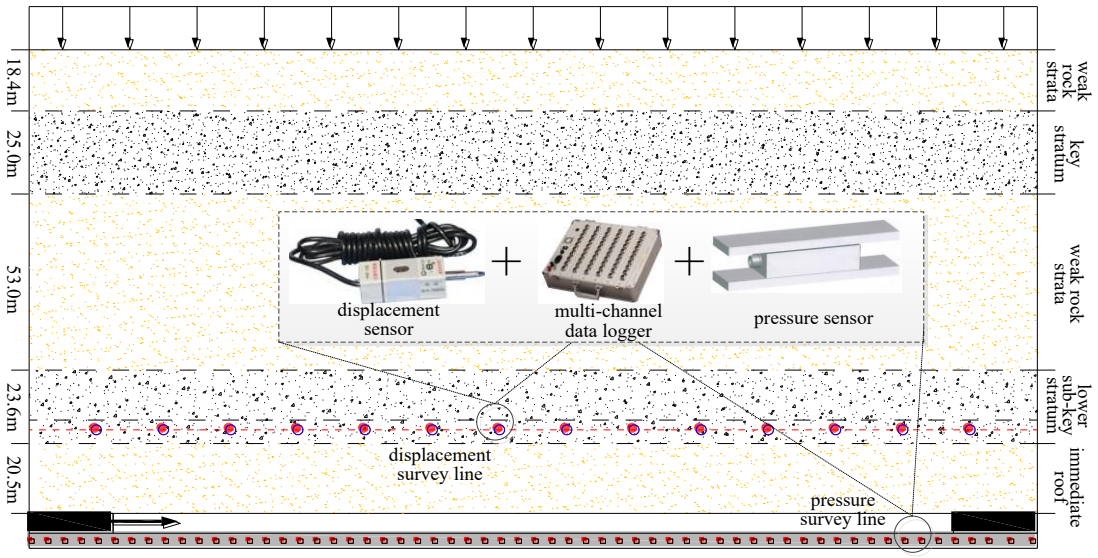



Figure 5 Layout of the model and measuring points

## 3.2 Movement law of mining-induced overburden failure

(1) Fracture and caving characteristics of mining-induced overburden

The working face was mined from the open-off cut to a distance of 188.3 m, and then the mining was completed. The roof experienced 7 times of fracture and caving successively, with the caved zone developing to a height of 20.5 m, a caving angle of 53°–67°, and the fractured zone developing to a height of 90.5 m. The mining-induced overburden exhibited obvious characteristics of "three horizontal zones" and "three vertical zones", and the fractured zone was wider at the bottom and narrower at the top, showing a trapezoidal distribution. With the advance of the working face, influenced by the fracture movement of the lower key stratum, the caved rock mass in goaf presented a dynamic evolution process of "caving bulking—deformation contraction—full compaction". Moreover, the progressive compaction of the caved rock mass and its bearing mechanical characteristics also affected the movement of the block structure of the lower key stratum. Therefore, the formation and evolution of the caved zone is the basis for the damage and failure of the overlying "two zones". The severity of the overburden failure movement decreases with the decrease in mining depth, i.e., the mining-induced damage gradually attenuates during its upward transmission from bottom to top, as shown in Figure 6.

Controlled by the thick and hard rock strata, the overburden subsidence or damage transmission has a time-dependent nature, and finally forms the "three zones" characteristics and the corresponding three types of rock mass structures:

① The strata in the caved zone suffer the greatest damage and failure, and are mainly dominated by granular and fragmented structures. The caved rock blocks vary in size and are disorderly accumulated. In comparison, the irregular arrangement characteristics in the lower part of the caved zone are more obvious, with smaller block sizes; in the upper regular caving zone, the strata connecting with the voussoir beam structure of the lower key stratum cave while maintaining their original horizon, with larger blocks and larger voids between blocks, showing overall compaction and shrinkage deformation characteristics.

② Block structures are formed in the fractured zone, with the blocks hinged to each other and possessing a certain bearing capacity. Owing to the supporting action of the coal mass at the mining

boundary, the strata in the fractured zone near the mining boundary have a smaller overall subsidence. The fractured rock blocks of the lower key stratum bite with each other to form a voussoir-beam half-arch structure, with larger voids in its lower part, exhibiting instability deformation characteristics of block structures.

③ The strata in the sagging zone are relatively complete with fewer fractures, and have the smallest overall deformation and damage.

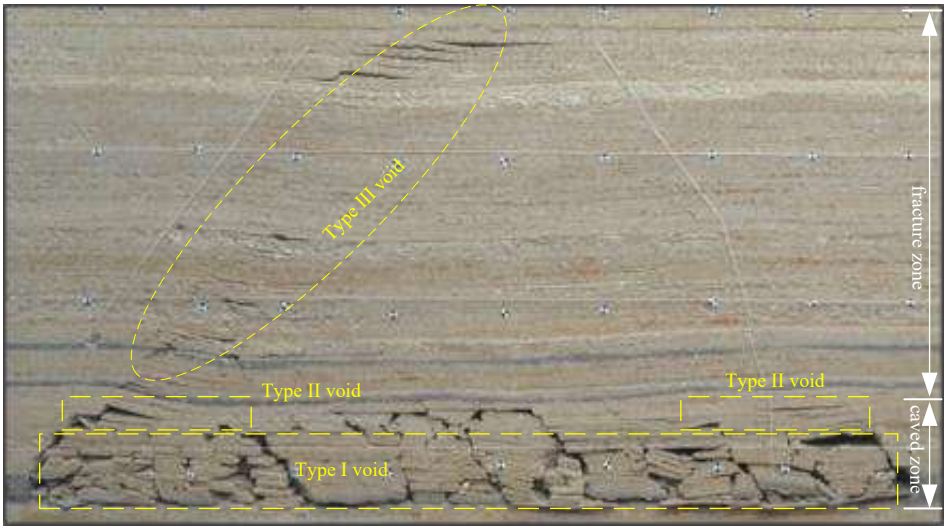



Figure 6 Roof fracture movement image when the working face advances to 188.3 m

(2) Spatial distribution and scale of voids in goaf

With the advance of the working face, the movement characteristics of "blocks" formed by the periodic fracture of the overlying hard rock strata were comprehensively reflected. The fractured rock blocks form a "voussoir beam" structure, which dominates the rock mass movement. As shown in Figure 6, the rock mass fracture and block movement inevitably lead to the formation and variation of new voids, manifested in two ways: the generation of new voids by roof caving bulking, and the dynamic variation of existing voids. These two ways alternately become dominant with the roof fracture movement, resulting in great differences in rock mass structure and void development at different positions. According to the spatial distribution and scale of the voids, they are divided into four types:

① Type I voids: after the caving of the immediate roof, the discontinuous and non-uniformly distributed cavity-type voids generated between the caved gangue piled up in granular and fragmented structures. They are generally more distributed at the mining boundary, coal pillars and insufficiently compacted areas. Except for the boundary area, the strata in the upper part of the caved zone, under the bulking and filling action of the caved rock mass below, fracture with a larger fragmentation degree and a relatively regular block arrangement. Because the bulking condition is insufficient, the strata fracture and cave without producing obvious dislocation and cavity-type voids, i.e., fracture and caving occur but have not expanded to form large-scale voids.

② Type II voids: the "O"-ring voids formed in the lower part after the lower key stratum of the main roof fractures to form the voussoir beam structure. Interacting with the caved rock mass, a larger void space exists, which is generally prominently developed at the mining boundary and periodic weighting positions.

③ Type III voids: the block structures formed by the asynchronous fracture movement of the upper strata of the main roof, in which the blocks bite and hinge with each other; fracture fissures formed between blocks, as well as bedding separation gaps formed by the incoordinate deformation between the main key stratum and subkey strata and between subkey strata.

④ Type IV voids: fractures, pores, joints and cavities originally developed in the roof strata, and this part of voids will expand and contract during the rock mass movement.

From the perspective of spatial distribution, these voids are formed and distributed from bottom to top in the strata of the caved zone and the fractured zone, showing a certain regularity, but with great differences in void scale. Among them, Type I and Type II voids are the voids in the caved zone, which increase and gather in the horizontal direction from the middle of the caved zone toward the mining boundary, but differ greatly at different mining time stages. From the perspective of void characteristics, the voids generated by bulking in the caved zone are larger than the original voids inside the strata by multiple orders of magnitude in scale and size. The long-term existence of these bulking voids will further prolong the instability movement of the overburden structure and the surface subsidence.

## 3.3 Dynamic evolution law of voids in the caved zone

(1) Periodic roof caving and void development in the caved zone

To quantitatively describe the dynamic evolution law of voids in the caved zone, the ImageJ software was used to conduct binarization processing, measurement and statistics on the model images, so as to obtain the void development degree in the caved zone and the quantitative information of its evolution with the periodic roof caving, as shown in Figure 7.

The void cross-sectional area (the total area of voids in the caved zone measured on the physical model surface), the void ratio (the ratio of the void cross-sectional area to the cross-sectional area of the caved zone on the physical model surface), and the ratio to the mined-out space (the ratio of the void cross-sectional area to the excavated area on the physical model surface) were adopted as the quantitative description indicators of void development in the caved zone. The void development indicators of the goaf after each roof caving were statistically analyzed, and the results are shown in Table 2.

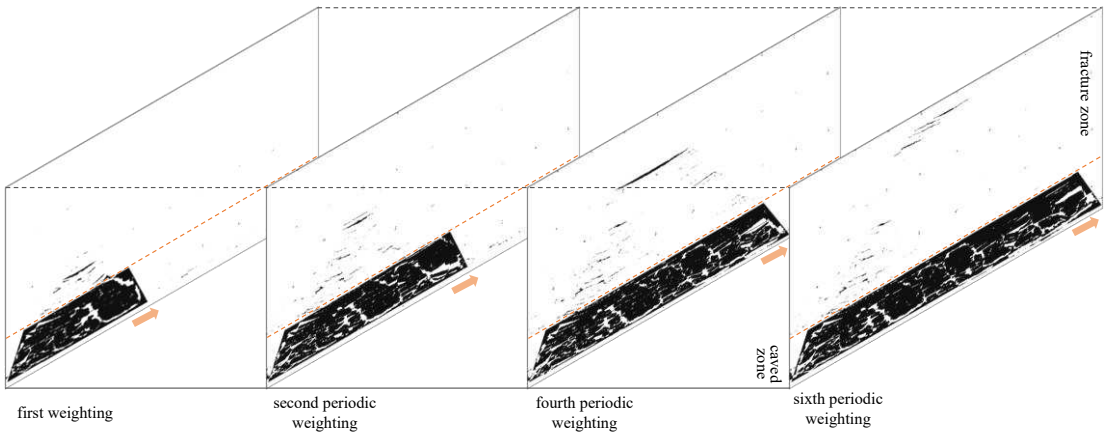



Figure 7 Evolution process of voids in the caved zone during periodic roof caving

Table 2 Dimensions of the caved zone and internal void parameters during periodic roof caving

| Roof caving sequence | Dimensions of the caved zone | Void parameters of the caved zone |
|---|---|---|

| | Length /m | Cross-sectional area/m$^2$ | Cross-sectional area/m$^2$ | Increment /m$^2$ | Void ratio /% | Ratio to mined-out space/% |
|---|---|---|---|---|---|---|
| 1 | 82 | 1631.21 | 218.22 | - | 13.38 | 44.35 |
| 2 | 101.8 | 2149.97 | 325.06 | 106.84 | 15.12 | 53.22 |
| 3 | 116 | 2522.01 | 367.24 | 42.18 | 14.56 | 52.76 |
| 4 | 136 | 3046.01 | 423.78 | 56.54 | 13.91 | 51.93 |
| 5 | 157 | 3596.21 | 527.83 | 104.05 | 14.68 | 56.03 |
| 6 | 172.5 | 4002.31 | 544.46 | 16.62 | 13.60 | 52.60 |
| 7 | 188.3 | 4416.27 | 588.92 | 44.46 | 13.34 | 52.13 |

Accordingly, the accumulation morphology of the caved gangue and the spatial distribution characteristics of voids during rock mass movement were obtained:

① Within a certain range at the open-off cut, the stopping line and behind the working face, the caved gangue is loosely accumulated, with more cavity-type voids distributed and a larger void scale, the maximum being 10.7 × 3.6 m (length × width). The voids at the boundary are mainly related to the overhanging length and bending degree of the immediate roof. From the perspective of vertical distribution, the particle size of the gangue rock blocks in the lower part of the caved zone is relatively small, with more voids distributed between the caved rock blocks; in the upper part of the caved zone, since the caved gangue is accumulated regularly, fewer voids develop.

② At the boundary, "O"-ring voids are distributed in the region where the lower part of the first rotation rock block in the voussoir beam structure of the lower key stratum has not fully contacted the caved gangue, with a maximum void size of 17.4 × 2.9 m. With the movement of the block structure, this part of the voids contracts obviously, and the void length and width are controlled by the length and angle of the rotation rock block.

③ The voids behind the working face gradually shrink and decrease with the increase in the distance lagging behind the working face. Affected by the difference in roof caving steps, the newly increased void cross-sectional area in the caved zone after periodic roof caving is 16.62–106.84 m², and the cumulative void cross-sectional area basically increases linearly with the increase in the caved zone size, as shown in Figure 8.

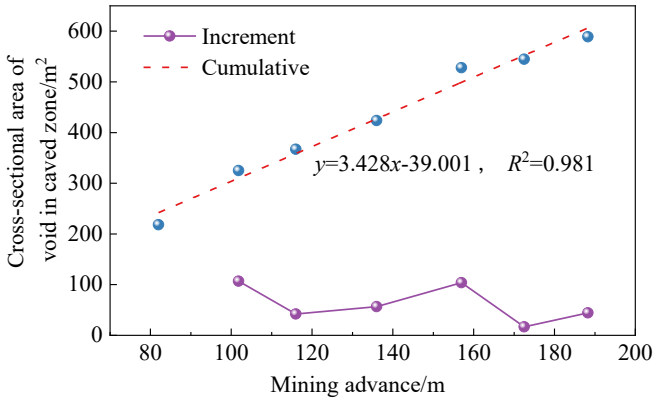



Figure 8 Increment of voids in the caved zone during the advancing process of the working face

④ Through statistical analysis of the variation law of voids in the caved zone during the advancing process of the working face, the void ratio of the caved zone was obtained as 13.34%–15.12%, and the ratio of the total void cross-sectional area to the mined-out space in the caved zone was 44.35%–56.03%, as shown in Figure 9.

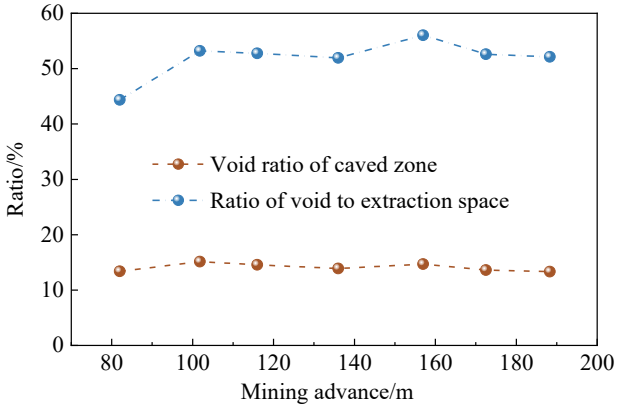



Figure 9 Variation law of voids in the caved zone during the advancing process of the working face

(2) Influence of overburden structure movement on the dynamic evolution of voids in the caved zone

① The movement of the lower key stratum has a significant influence on the generation, development and spatiotemporal distribution of voids in the caved zone. As shown in Figure 10, along the advancing direction of the working face, the zonal differentiation of voids in the caved zone is significant, exhibiting a three-stage development law with the fracture movement of the lower key stratum: before the fracture of the lower key stratum, the voids enter an active development stage and reach the maximum at the moment of imminent fracture; during the fracture and subsidence of the lower key stratum, they enter a compaction and contraction stage; after the block structure of the lower key stratum tends to be stable, they enter a stable stage. The local voids in the caved zone, with the process of "caving bulking—deformation contraction—full compaction" of the caved rock mass, show a law of increasing first, then decreasing and finally tending to be stable, and a large number of voids always exist on both sides of the caved zone.

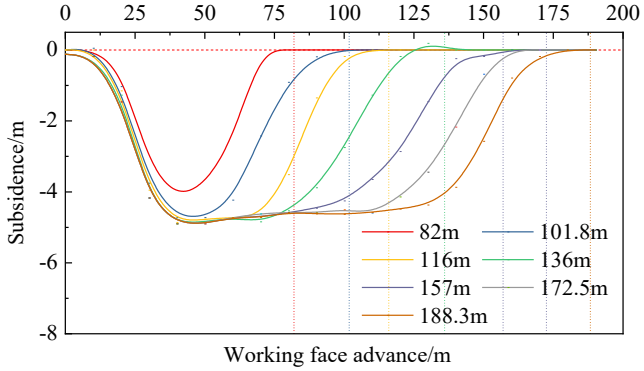



Figure 10 Fracture subsidence curve of low key strata

② With the increase in the distance lagging behind the coal wall, the voids in the caved zone gradually decrease and tend to be stable after reaching a certain distance. As shown in Figure 11, the void variation in the observation area (the observation area boundary is 61.5–101.8 m away from the open-off cut, with an observation area of 906.35 m²) during the advancing process of the working face was recorded. It was found that the dynamic evolution of voids in the observation area is closely related to the development and evolution of the half-arch structure above the coal wall of the working face, and changes dynamically with the periodic forward movement of the half-arch structure. Within the range of 0–34.2 m from the coal wall, the observation area is located in the pressure-relief zone below the half-arch structure, where the void volume in the caved zone is large

and tends to decrease with the increase in the distance from the coal wall (the front arch foot). Beyond the position 34.2 m away from the coal wall, the observation area is located at the arch foot or outside the arch of the half-arch structure, where the voids tend to be stable.

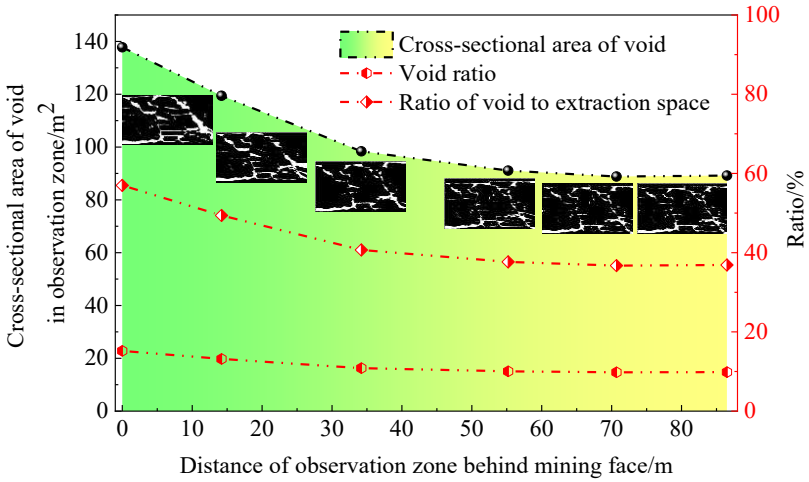



Figure 11 Variation law of voids in the observation area with the advance of the working face

(3) Influence of floor stress of the caved zone on the dynamic evolution of voids in the caved zone

The floor stress of the caved zone is a comprehensive reflection of the mining-induced overburden structure and its evolution process. In this test, the vertical stress data of the floor in the caved zone were collected, and the stress concentration factor was used to characterize the stress recovery of the caved rock mass during the formation of the caved zone, so as to further verify the influence law of overburden structure movement on the voids in the caved zone. As shown in Figure 12, the distribution curves of the stress concentration factors at each measuring point on the stress survey line when the working face advanced to 172.5 m are presented. It can be seen from the Figure that the floor stress of the caved zone changes in three stages, and the specific process is analyzed as follows:

① Within a range of about 35 m behind the working face, i.e., the pressure-relief zone protected by the half-arch structure, the overburden load is transferred to both sides and downward through the half-arch structure, thereby reducing the force directly acting on the caved gangue. This region is the naturally accumulated zone of the caved gangue, where the floor is only subjected to the self-weight of the caved gangue, and the voids show an increasing trend, corresponding to the active development period of voids.

② At a distance of about 35–45 m behind the working face, the interaction stage between the key block and the caved gangue is entered, i.e., the arch-foot position of the half-arch structure. The "large deformation" characteristics of the key block are obvious, and the load transfer effect is significant. The stress transfer and evolution of the block structure will change the compactness of the rock mass in the caved zone behind the pressure-relief zone, and the voids in the caved zone enter the compaction and contraction period with the movement of the structure, which also confirms that the void evolution in the caved zone is controlled by the half-arch structure effect.

③ Beyond about 45 m behind the working face, the key block completely contacts the gangue and reaches equilibrium, and the vertical stress of the floor gradually recovers to the level of the in-situ rock stress and tends to be stable, corresponding to the stable period of the voids in the caved zone. However, a part of the voids is still retained inside. Under the disturbance of external

conditions, the gangue in the caved zone will still produce progressive deformation, and the overburden and the ground surface will still produce progressive deformation damage.

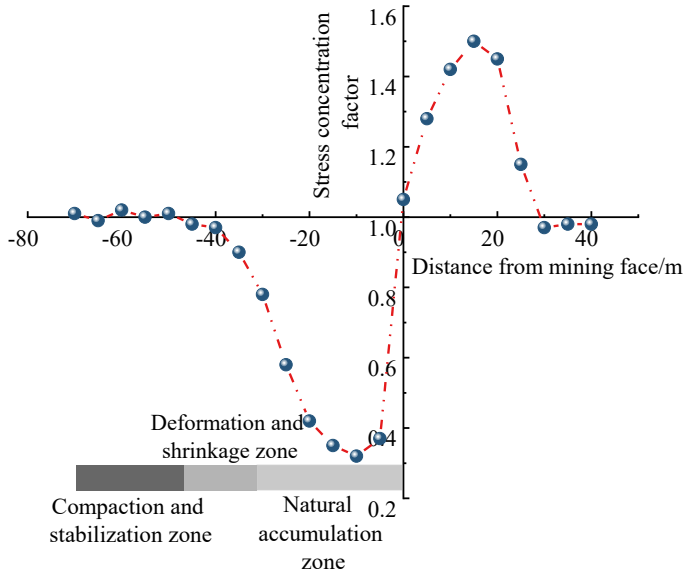



Figure 12 Distribution curves of the vertical stress concentration factor on the floor

In summary, the spatiotemporal evolution of voids in the caved zone is highly coupled with the fracture movement of the lower key stratum and the stress distribution law of the floor, and also exhibits an obvious three-stage variation characteristic. Overall, it presents the basic characteristics of significant zonal differentiation, prominent boundary effects and obvious control by overburden movement; moreover, the roof structure movement and stress transfer are the direct inducements driving the dynamic variation of voids in the caved zone.

# 4 Analysis of damage mechanism of voids in goaf

## 4.1 Damage composition

The mining-induced damage degree is transferred and attenuated step by step from the mining space from bottom to top, which is an extremely complex four-dimensional problem varying with time and space, and the mining-induced damage does not stop immediately when the mining ends. In the study of mining subsidence, the surface movement process caused by mining is divided into the initial period, active period and decay period [24], as shown in Figure 13.

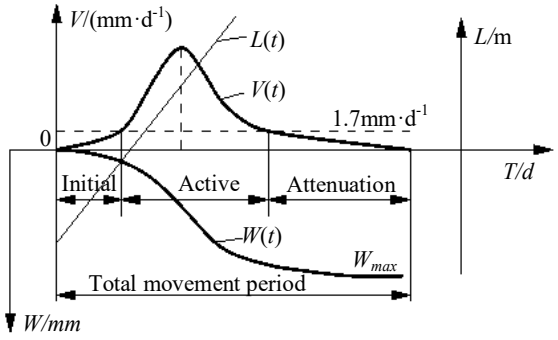



Figure 13 Duration of surface movement

According to the stages in which the overburden and surface movement deformation occurs, it can be divided into two parts [25]: the first part is the movement caused by the variation of the mining space, accounting for about 65%–75% of the mining thickness; the second part is the movement

that occurs with time after the mining ends, which is mainly the overall movement and damage of the overlying strata caused by the deformation and contraction of the bedding separation space in goaf and various voids in the caved zone, being a continuous and gradual process. Among them, the movement from the end of mining to before the surface is considered to tend to be stable (the surface subsidence is less than 30 mm for six consecutive months) according to the *Coal Mine Safety Regulations* accounts for 8%–15% of the mining thickness; the remaining movement is the residual movement deformation that gradually changes with time, accounting for 15%–20% of the mining thickness.

## 4.2 Damage mechanism of voids in goaf

After the mining ends, since the goaf is occupied by mutually stacked broken rock masses and a large number of voids, the spatial structure is extremely unstable. When external conditions change, this relatively stable spatial structure is broken due to the re-compaction deformation of the caved gangue, causing the overall continuous damage of the overburden, which is called the "void damage effect" of the caved zone. Owing to this effect, the overlying strata will experience a periodic and staged evolution process of "instability—stability—re-instability—re-stability". According to the generation characteristics of the continuous deformation damage of the overburden, it can be divided into two types: inducing the continuous large deformation damage of the lower key stratum structure, and generating residual subsidence damage.

(1) Inducing the continuous large deformation damage of the lower key stratum structure

Near the mining boundary, the roof strata form a "cantilever beam + voussoir beam" structure as the load-bearing main body to control the stability of the overburden. In this region, there are a large number of uncaved spaces and insufficiently compacted spaces that may cause the instability of this secondary half-arch bearing structure, which is called the deformation space for the continuous damage of the overburden structure. Moreover, the smaller the width of the caved zone, the longer the cantilever and the less sufficient the roof caving, the larger the deformation space causing the continuous damage of the overburden structure. Since the deformation space below the upper main key stratum is significantly smaller than that below the lower key stratum, its stability is higher than that of the lower key stratum. Therefore, only the influence of the deformation space in the caved zone on the instability of the lower key stratum structure is analyzed. For the instability of the lower key stratum structure, its "S–R" (slip and rotation) instability should usually be considered, and the influence of coal pillar failure should also be considered, which is specifically divided into the following three cases:

① "S–R" instability of the lower key stratum

During the mining process, with the formation of the caved zone, the mining-induced overburden maintains a relatively stable state. At this time, the structure of the lower key stratum conforms to the "S–R" model of the voussoir beam structure, and the stability of the key block determines the stability of the whole "voussoir beam" structure. The variation of the structural deformation space increases the possibility of the "large deformation" movement of the key block. Under the condition of a small depth-thickness ratio (the ratio of mining depth to mining thickness), the "large deformation" of the key block will simultaneously cause severe non-uniform subsidence of the ground surface. Taking the bulking factor to characterize the influence of voids in the caved zone on the "large deformation" of the key block, the influence relationship is as follows:

$$Z_1 = M - \sum h\left(K_p - 1\right) \tag{2}$$

where $Z_1$ is the subsidence of the first key block, in m; $\sum h$ is the total thickness of the immediate roof, in m; $M$ is the mining thickness, in m; and $K_p$ is the bulking factor of the caved rock mass.

② Coal pillar failure inducing the instability of the lower key stratum

The instability failure of the coal pillar will inevitably lead to the instability of the equilibrium structure of the hinged blocks of the lower key stratum, causing it to be in a continuous deformation state, and then inducing the "S–R" instability. This situation is extremely unfavorable to the control of the overburden, which not only aggravates the overburden failure but also prolongs the stability period of the overburden. Based on the A. H. Wilson two-zone confinement theory and the empirical formula method, the condition for maintaining the stability of the coal pillar is as follows [26]:

$$a_m \geq 2r_p + r_e \tag{3}$$

where $a_m$ is the width of the coal pillar, in m; $r_p$ is the width of the yield zone of the coal pillar, in m; and $r_e$ is the width of the elastic core zone of the coal pillar, in m.

The width of the yield zone of the coal pillar, $r_p$, is:

$$r_p = \frac{MA\mathrm{d}}{2\tan\varphi_0}\ln\left(1+\frac{k_0\gamma H_m\cos\alpha}{c_0}\tan\varphi_0\right) \tag{4}$$

where $M$ is the thickness of the coal seam, in m; $H_m$ is the buried depth of the coal pillar, in m; $\alpha$ is the dip angle of the coal seam, in °; $A$ is the lateral pressure coefficient; $\varphi_0$and $c_0$ are the internal friction angle and cohesion at the interface between the coal mass and the rock stratum, in ° and MPa, respectively; $\gamma$ is the average unit weight of the overlying strata, in kN/m³; $k_0$ is the stress concentration factor; and $d$ is the mining disturbance factor, which is determined to be 1.5–3.0 in field measurement.

According to the stability theory, the core zone ratio should satisfy:

$$\rho = \frac{a_m - 2r_p}{a_m} \tag{5}$$

According to the roof caving characteristics, there are often large cavity voids near the coal pillar side, which makes it difficult to provide lateral pressure for strengthening the coal pillar. Moreover, when both sides of the coal pillar are mined out, long-term deterioration effects such as water erosion and natural weathering will further aggravate the instability failure of the coal pillar.

③ Fracture line overlapping inducing the instability of the lower key stratum

Reference [27], using the field microseismic monitoring method, has confirmed that when the coal pillar cannot effectively isolate the connection and influence between two goaf areas, the lower key stratum of the adjacent goaf will rotate and slide to produce secondary instability under the mining-induced influence of the current working face. According to the mine pressure theory, the fracture line of the main roof strata occurs in the coal wall. Calculating the position of the fracture line according to the location of the maximum bending moment of the main roof, the distance between the fracture line and the coal wall is [28]:

$$l_d = \frac{\tan^{-1}\left[\dfrac{\beta\left(2\alpha M_0 s + rQ_0\right)}{r^2 M_0 + \alpha r Q_0}\right]}{\beta} \tag{6}$$

$$\beta = \left(\frac{\sqrt{k_w/EI}}{2} + \frac{N}{4EI}\right)^{1/2} \quad \alpha = \left(\frac{\sqrt{k_w/EI}}{2} - \frac{N}{4EI}\right)^{1/2}, \quad s = N/EI, \quad r = \sqrt{k_w/EI}$$

where $l_d$ is the distance between the fracture line and the coal wall, in m; $k_w$ is the Winkler foundation coefficient; $EI$ is the flexural rigidity of the rock beam of the lower key stratum, in N·m²;

and $M_0$, $Q_0$and $N$ are the internal forces of the section at the coal wall (x = 0), i.e., the bending moment, shear force and axial force, in N,N·m, N and N, respectively.

From the above equation, it can be seen that the position of the fracture line of the lower key stratum is mainly related to the properties of the immediate roof and the coal wall. Therefore, to ensure that the coal pillar can effectively isolate the goaf areas on both sides, the minimum width of the coal pillar should satisfy $a_m \geq 2l_d$.

Based on the analysis of the above three aspects, the method of backfilling the caved zone can be adopted to eliminate the continuous deformation space of the lower key stratum structure, so as to improve the stability of the lower key stratum and avoid the continuous large deformation damage of the structure caused by its own instability, the deformation failure of the coal pillar and the overlap of fracture lines.

(2) Generating residual subsidence damage

Reference [29] refers to the surface subsidence within decades after the mining ends, starting from the beginning of prediction (or the construction of building facilities), as "residual subsidence". The residual subsidence damage still cannot be ignored. In this process, besides the additional stress caused by the change of external conditions, the factors leading to residual subsidence mainly include the compaction and contraction deformation of voids in the caved zone and the closure of bedding separation spaces in the fractured zone, among which the damage after the contraction deformation of voids in the caved zone is dominant. Specifically:

① Long-term creep of the caved rock mass: due to the irreversibility of the granular and fragmented structures in the caved zone, the voids in this region will also exist for a long time. Under the influence of external conditions and time, the granular and fragmented structures will undergo long-term slow creep and contraction, causing the overburden to produce re-subsidence, but the subsidence is small and relatively uniform; when the mining depth is large, it generally manifests as slow and continuous residual subsidence damage. The external influences mainly include the overburden load, as well as the compaction and contraction deformation caused by the weathering and strength attenuation of the rock mass in the caved zone under the action of groundwater and air.

② Instability of the "cantilever beam + voussoir beam" structure: the mining of adjacent working faces (layers) and the failure of coal (rock) pillars will break the relatively stable structure of the "cantilever beam + voussoir beam", which usually also causes the instability of the key block, leading to the "activation" movement of the overburden structure and producing new failure and damage. Among them, the voids in the caved zone are the main spatial source for the "activation" of the overburden structure, and are re-compressed greatly during the secondary movement of the overburden. This kind of damage phenomenon generally occurs more in the cantilever control area and the key block support area.

③ External disturbance: under external disturbances such as earthquakes, tectonic stress and ground buildings, the roof structure will be "activated" to move again under the additional stress.

# 5 Conclusions

(1) Through transient electromagnetic (TEM) detection tests, the electrical response characteristics of the goaf at the test working face were systematically obtained, and the spatial position and morphological development law of the void anomaly zones were clarified. Based on

the inversion results of the electrical parameters of the overburden, it was revealed that the void development degree in the longwall goaf decreases with the increase in the vertical distance from the coal seam following a polynomial function.

(2) Physical model tests confirmed that the development and evolution of voids in longwall goaf are controlled by the movement and deformation of the overburden structure, presenting continuous dynamic evolution characteristics in the spatiotemporal dimension, which leads to significant differences in the stress environment in different areas of the goaf and is the core reason for the heterogeneity of the spatial distribution of voids. The test quantitatively analyzed the spatial distribution range and development degree of voids in the caved zone, as well as their evolution law with the periodic fracture of the lower key stratum. The results show that the spatiotemporal evolution of voids in the caved zone is highly coupled with the fracture movement of the lower key stratum and the stress distribution law of the floor; the caved zone generally presents the basic characteristics of significant zonal differentiation, prominent boundary effects and obvious control by overburden movement, and the roof structure movement and stress transfer are the direct inducements driving the dynamic variation of voids in the caved zone.

(3) Based on the results of transient electromagnetic detection and physical model tests, it is considered that the voids in the caved zone are the deformation space for the continuous instability of the roof structure, and their damage effects are mainly manifested in two aspects: one is inducing the continuous large deformation of the lower key stratum structure, and the other is generating residual subsidence damage. The occurrence mechanisms of continuous large deformation damage were systematically clarified, including the "S–R" instability of the lower key stratum, and the instability of the lower key stratum induced by coal pillar failure and the overlap of fracture lines; as well as the occurrence mechanisms of residual subsidence damage, including the long-term creep of the caved rock mass, the instability of the "cantilever beam + voussoir beam" structure, and external disturbance.

**Funding:** This research was funded by the National Natural Science Foundation of China, grant number No. 52664017 and No. 52664016, the Natural Science Foundation of Inner Mongolia of China, grant number No. 2025MS05068 and No. 2026MS0500, the Basic Scientific Research Operating Expenses Project of Universities Directly Affiliated to Inner Mongolia Autonomous Region, grant number No.2025QNJS005, and the Keju Plan of Inner Mongolia University of Science and Technology,grant number No.KJJH2024919.

**Acknowledgments:**This work was supported by the National Natural Science Foundation of China (Grant Nos. 52664017 and 52664016), the Natural Science Foundation of Inner Mongolia of China (Grant Nos. 2025MS05068 and 2026MS0500), the Basic Scientific Research Operating Expenses Project of Universities Directly Affiliated to Inner Mongolia Autonomous Region (Grant No. 2025QNJS005), and the Keju Plan of Inner Mongolia University of Science and Technology (Grant No. KJJH2024919). We thank the academic editors and anonymous reviewers for their kind suggestions and valuable comments.

**Availability data and materials:** The authors confirm that the data supporting the findings of this study are available within the article.

**Conflicts of Interest:** The authors declare no conflict of interest.

# References

[1] Energy Institute. Statistical Review of World Energy 2026[R]. London: Energy Institute, 2026.

[2] Yang, K., Feng, X. W., He, X., et al. (2026). Spatial dynamic evolution process of overburden rock mining and coal-based solid waste grouting and filling practice. Coal Science and Technology, 54(1), 84–99.

[3] Li, L., Huang, Q. X., Zuo, X., et al. (2022). Study on the Slurry Diffusion Law of Fluidized Filling Gangue in the Caving Goaf of Thick Coal Seam Fully Mechanized Caving Mining. Energies, 15(21), 8164.

[4] Xu, J. L. (2020). Research and progress of coal mine green mining in 20 years. Coal Science and Technology, 48(9), 1–15.

[5] Yuan, L. (2016). Strategic thinking of simultaneous exploitation of coal and gas in deep mining. Journal of China Coal Society, 41(1), 1–6.

[6] Li, S. G., Lin, H. F., Zhao, P. X., et al. (2014). Dynamic evolution of mining fissure elliptic paraboloid zone and extraction coal and gas. Journal of China Coal Society, 39(8), 1455–1462.

[7] Xu, J. L., Zhu, W. B., Xuan, D. Y., et al. (2025). Thought of full-stratigraphy and its practice in ground control. Journal of China Coal Society, 50(1), 166–179.

[8] Wang, B. F., Lyu, Y. H., & Zhang, J. (2025). Zone feature and control technology of overlying strata mining-induced fracture in shallow buried compound goaf. Coal Science and Technology, 53(2), 41–52.

[9] Li, H. Y., Wang, W. H., Qi, Q. X., et al. (2014). Study on fissure development rule of overlying strata influenced by mining based on fractal theory. Journal of China Coal Society, 39(6), 1023–1030.

[10] Zhang, H. Z., Deng, K. Z., & Gu, W. (2016). Distribution law of the old goaf residual cavity and void. Journal of Mining & Safety Engineering, 33(5), 893–897.

[11] Hu, S. Y., Han, D. D., Feng, G. R., et al. (2020). The effect of stress transfer on the spatial distribution of void ratios in crushed rock mass. Journal of Mining & Safety Engineering, 37(4), 723–730.

[12] Zhang, C., Zhao, Y. X., & Bai, Q. S. (2022). 3D DEM method for compaction and breakage characteristics simulation of broken rock mass in goaf. *Acta Geotechnica*, *17*(7), 2765–2781.

[13] Hu, S. Y., Han, D. D., Feng, G. R., et al. (2020). Influence of stress on void ratios of compacted crushed rock masses in coal mine gobs. Natural Resources Research, 29(2), 1361–1373.

[14] Wolf, K. H., & Bruining, H. (2007). Modelling the interaction between underground coal fires and their roof rocks. Fuel, 86(17–18), 2761–2777.

[15] Miao, X. X., Li, S. C., & Chen, Z. Q. (2009). Bifurcation and catastrophe of seepage flow system in broken rock. Mining Science and Technology (China), 19(1), 1–7.

[16] Deng, K. Z., Tan, Z. X., Zhang, H. Z., et al. (2012). Research on calculating method of residual subsidence of longwall goaf. Journal of China Coal Society, 37(10), 1601–1605.

[17] Feng, G. R., Yan, Y. G., Yang, S. S., et al. (2009). Analysis on the damage zone of overlying strata and safety layer distance on the upward mining above the longwall goaf. Journal of China Coal Society, 34(8), 1032–1036.

[18] Li, Q. S., Guo, J. T., Zhang, K., et al. (2021). Damage conduction mechanism and key technologies of damage reduction in sources for intensive coal mining in Western China. Journal of China Coal Society, 46(11), 3636–3644.

[19] Qu, Q. D., Yao, Q. L., & Li, X. H. (2010). Research on theory of space conservation for subsidence control in backfill mining and its application. Journal of Hunan University of Science and Technology(Natural Science Edition), 25(1), 8–12.

[20] Guo, W. B., Xu, S. G., Yang, W. Q., et al. (2025). Distribution pattern of overburden void ratio induced by mining in goaf areas and corresponding zoning-based control measures. Journal of China Coal Society, 50(S2), 820–833.

[21] Yang, K., Feng, X. W., He, X., et al. (2026). Dynamic evolution process of overburden strata in thick coal seam backfill mining and engineering practice of coal-based solid waste grouting backfilling. Coal Science and Technology, 54(1), 84–99.

[22] Chen, S. J., Zhang, L. B., Jiang, N., et al. (2022). A case of large buildings construction above old-mine goaf in Shandong Province. Journal of China Coal Society, 47(3), 1017–1030.

[23] Guo, G. L., Deng, K. Z., Wang, H. Y., et al. (2000). Research on the mechanism and treatment measures of foundation instability above the mined-out area. Mine Pressure and Roof Management, (3), 39–42.

[24] Yu, X. Y., & Zhang, E. Q. (2010). Mining damage science. Beijing: China Coal Industry Press.
[25] Kang, J. R., & Zhao, Y. S. (2005). Analysis of subsidence ratio of strata and surface varying with time after mining stop by experiment. Journal of Liaoning Technical University(Natural Science), 24(3), 324–327.
[26] Wu, L. X., Wang, J. Z., & Guo, Z. Z. (2000). Basis of coal pillar design and monitoring. Xuzhou: China University of Mining and Technology Press.
[27] Wei, D., He, H., Qin, Y. F., et al. (2010). Study on mechanism of mining tremor induced by key strata instability in the gob beside the working face. Journal of China Coal Society, 35(12), 1957–1962.
[28] Qian, M. G., & Shi, P. W. (2003). Ground pressure and strata control. Xuzhou: China University of Mining and Technology Press.
[29] Yu, X. Y., & Shi, W. G. (1996). Methods for predicting residual surface subsidence. Journal of Xi'an Mining Institute, (1), 1–4,27.